

A Mesoscale Analysis over South Florida for a High Rainfall Event

ROGER A. PIELKE

Center for Advanced Studies, Department of Environmental Sciences, University of Virginia, Charlottesville 22903

WILLIAM R. COTTON

Department of Atmospheric Sciences, Colorado State University, Fort Collins 80521

(Manuscript received 12 January 1976, in revised form 20 October 1976)

ABSTRACT

The meteorological data collected during the 1973 NOAA-EML Florida Area Cumulus Experiment was used to describe the mesoscale weather patterns on 4 August 1973. It was found that the high rainfall on this date was due to the superposition of a synoptic-scale disturbance and the normal shallow sea breeze convergence field. The synoptic disturbance was not resolved from the conventional synoptic analyses. On this date, the thunderstorm activity was highly correlated with the diurnal heating and apparently developed in favored regions related to both the sea breeze convergence zone along the west coast and to the larger scale disturbance. The surface wind and temperature patterns were found to be strongly controlled by the diurnal heating cycle, and by the occurrence or non-occurrence of showers. It is concluded that the reduction in lower level wind speed after a rain occurrence was a result of surface cooling causing a decoupling of the surface from the larger scale pressure gradient.

The analysis of cloud base vertical velocity and its variance illustrates a strong coupling between the mesoscale and the thermal scale in spite of the fact that spectral analysis indicated a marked scale separation between the thermal convective scale and its larger scale. The strong excursion of the slope of the vertical velocity energy spectrum from a $-5/3$ slope over the scale range of 0.2–0.8 km indicates that eddies on this scale range are a strong source of kinetic energy generation.

1. Introduction

It has become increasingly obvious that mesoscale atmospheric processes must be understood if we are to improve our ability to forecast and to properly describe the weather to industry, agriculture and the public. Circulations in the atmosphere on this scale, which directly influence local weather, include sea breezes, mountain-valley winds, drainage fogs, squall lines, and so forth. Each of these features is significantly influenced by the underlying terrain as well as the larger scale synoptic field.

The purpose of this study is to examine a particular weather episode, namely a high rainfall event over south Florida, where the synoptic fields appeared to be rather uniform and steady. The initial work of studying the south Florida mesoscale environment was begun by Byers and Rodebush (1948), Gentry (1950), Day (1953) and Gentry and Moore (1954), and was continued by the more recent work of Plank (1969), Gerrish, (1969) and Pielke (1973). The latter research involved the analysis and interpretation of observations over south Florida which included radar measurements along with conventional surface and upper air data. From this work it has been found that the sea breeze is the dominant weather feature over south Florida on most summer days.

Pielke (1974) and Cotton *et al.* (1976) attempted to mathematically simulate, with a three-dimensional mesoscale model, the sea breeze over south Florida during synoptically undisturbed conditions using existing standard weather stations and radar coverage to verify the model. The results demonstrated that, even without considering the dynamic and thermodynamic effects of cumulonimbus activity, the sea breeze is the dominant control on the preferred locations of cumulonimbus complexes over south Florida on synoptically undisturbed days.

Unfortunately, however, while the study provided new insight into the initiating and controlling influence on thunderstorm occurrence over south Florida, there were little data available to quantitatively verify the model. The routinely available surface data were too sparse to provide an adequate documentation of a sea breeze event, while the radar and satellite imagery could provide little more than a qualitative evaluation.

In the summer of 1973, the Florida Area Cumulus Experiment (FACE) was initiated by NOAA's Experimental Meteorology Laboratory (EML) to remedy some of the inadequacies of the standard observational network. This program was designed to evaluate the potential of dynamic seeding of cumulus congestus in order to promote their merger, with its attendant

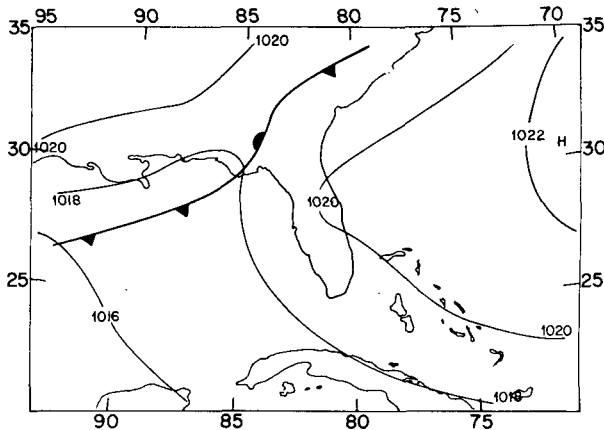


FIG. 1. Synoptic surface analysis at 0700 EST 4 August 1975.

multifold increase in rainfall (Simpson and Dennis, 1974). As a necessary component of this program, a mesoscale observational network was established. As shown by Cotton and Pielke (1976a), it is unlikely that an accurate evaluation of multiple cloud-seeding potential can be determined without an understanding of the mesoscale environment.

This paper uses the FACE observations to describe the mesoscale environment over south Florida on 4 August 1973. This date was chosen for analysis as a day representative of extensive cumulonimbus activity over south Florida, but where no synoptic disturbance was evident in the synoptic analyses [Fernandez-Partagas, Appendix A of Staff, EML (1974)].

The radar analyses (Woodley *et al.*, 1974) indicated that rainfall on this date in the EML target area¹ was well above the average for the period of the FACE program. In fact, out of 80 days in which digitized radar data were collected, only 11 had more rain in the EML target area for the period 0800 to 1700 EST.² This was the wettest day in which the FACE low-level aircraft collected mesoscale data with an average rainfall of slightly more than 1 cm recorded by the gage-

¹ See Cotton and Pielke (1976a, Fig. 3) for an illustration of the target area.

² Due to anomalous propagation at other times, rainfall rates were most accurate for the period 0800 to 1700 EST.

adjusted radar in the target area between 0800 and 1700. An analysis and interpretation of the mesoscale environment on this date may explain the high rainfall, as well as improve our understanding of the effects of extensive cumulonimbus convection on the sea breeze.

2. Observations

The observational information available for 4 August includes aircraft, satellite, radar, as well as surface and upper air observations.

a. Synoptic analysis

The synoptic analyses at the surface, 850, 700, 500 and 200 mb at 0700 EST³ for 4 August are given in Figs. 1-3. The lower and middle troposphere over south Florida appear dominated by a large anticyclone with its center well to the east of the state. At 200 mb, a large anticyclone lies off the southeast coast of the United States. The synoptic analyses at 1900 EST (see Cotton and Pielke, 1976b) for these same levels show a similar pattern with a large anticyclone at low and mid levels to the east of the peninsula and an upper level ridge off the Carolina coast. None of the analyses show any indication of a definable synoptic disturbance which could have caused the comparatively high rainfall on this date.

b. Surface, radar and satellite observations

The locations of surface observations, made at regular reporting stations, by cooperative observers and by mechanical weather stations, are plotted in Fig. 4. The regular reporting stations included sites of the National Weather Service (NWS), Federal Aviation Administration (FAA), and the Air Force, Navy and Coast Guard. Observation frequency ranged from continuous strip-chart recordings to once-a-day readings. The 29 cooperative observers (see Acknowledgment) who made observations with frequencies ranging from once a day to once an hour, volunteered from about 180 individuals

³ Prepared by the National Hurricane Center (surface and 200 mb) and Jose Fernandez-Partagas (850, 700 and 500 mb).

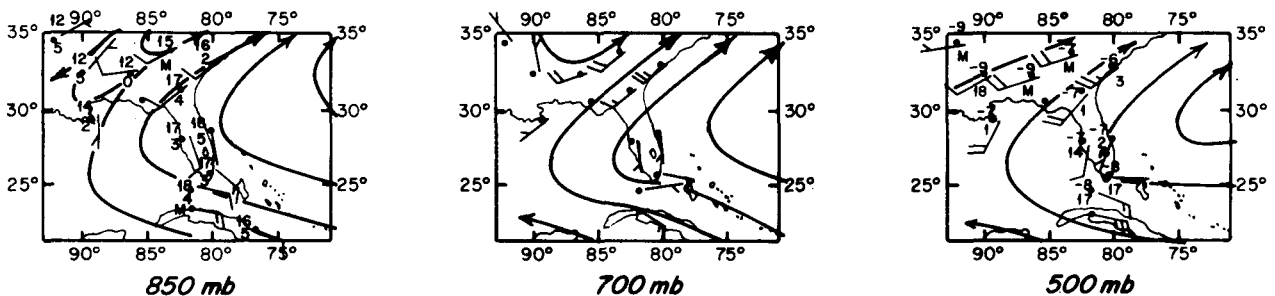


FIG. 2. 850, 700 and 500 mb analysis at 0700 EST 4 August 1973.

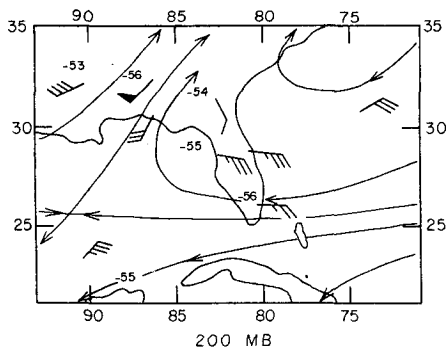


FIG. 3. 200 mb analysis at 0700 EST 4 August 1973.

whose support was solicited. Most of the observers recorded wind speed and direction, temperature and significant weather, although several reported only one of these. Their volunteer time and effort were crucial to the successful completion of this phase of the FACE program.

Five mechanical stations from the University of Virginia network (Staff, EML, 1974, p. 25) in the center and near the four apexes of their array were used to describe the area south of Lake Okeechobee, while ten mechanical weather stations, leased from Meteorology Research Incorporated, were placed at selected sites in order to fill voids in the data array. Maintenance of the mechanical weather stations, however, was often difficult. Unfortunately, LMR proved to be an unreliable station during the last half of the program because the clock on the station ran increasingly faster relative to actual time. Consequently, observations from this station on this date are questionable.

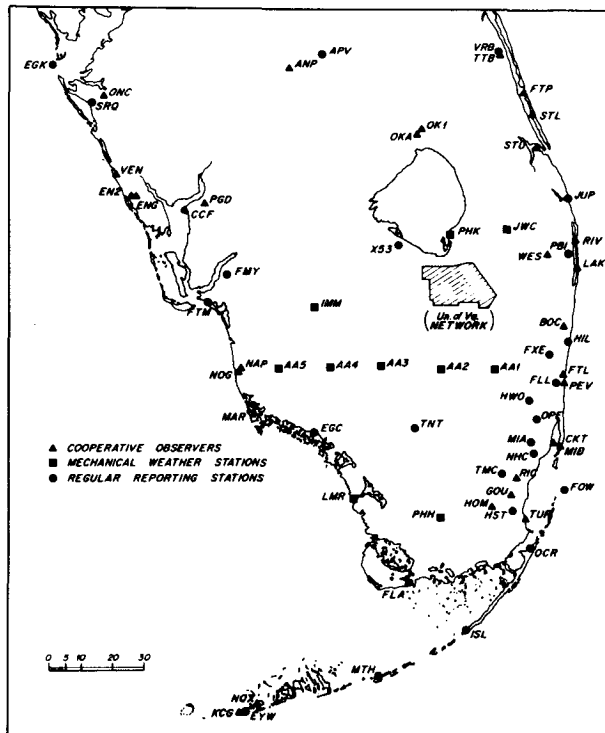


FIG. 4. Locations of Florida Area Cumulus Experiment (FACE) surface observations during 1973.

The hourly observed surface winds over south Florida for the period 0500 to 2000 EST on 4 August are given in Cotton and Pielke (1976b). In order to conserve space only a time cross section along a line from Fort Lauderdale (FTL) to Naples (NAP) is given in Fig. 5,

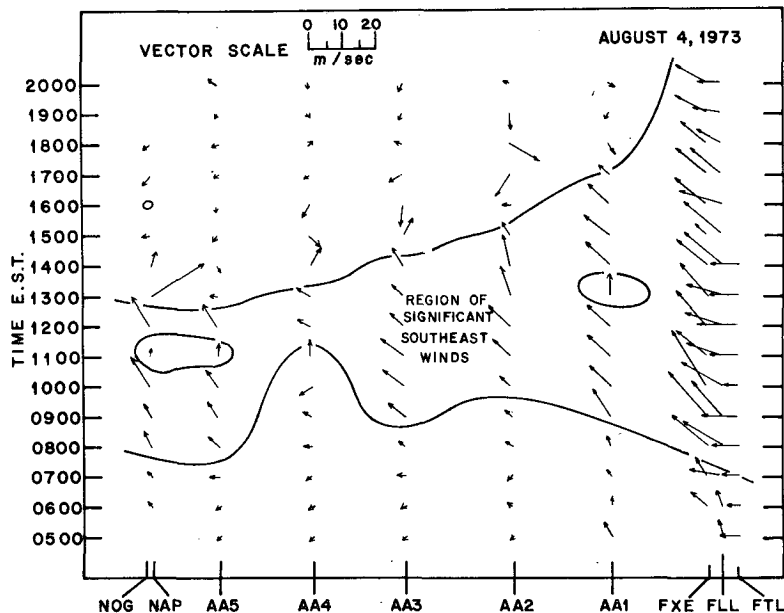


FIG. 5. The Naples to Fort Lauderdale time cross section of surface wind from 0500 to 2000 EST 4 August 1973.

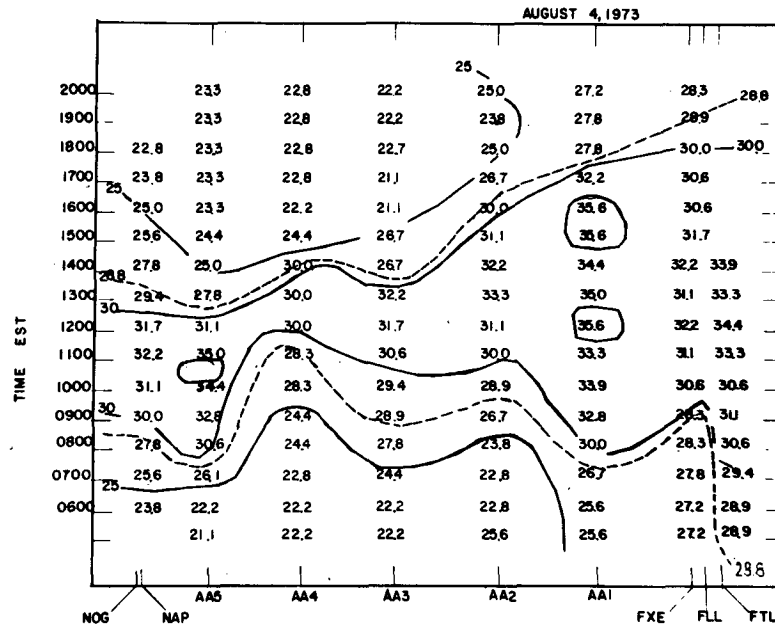


FIG. 6. As in Fig. 5 except for temperature.

and hourly maps of Miami WSR-57 digitized 10 cm radar data (Fig. 7-16) are presented here to illustrate the observed surface wind pattern.

The time cross sections were particularly useful in describing the observed surface wind and temperature patterns (Figs. 5 and 6) over south Florida. Several important features were found from these analyses:

1) The winds in the early morning (primarily before 0800-0900), away from the immediate east coast, were quite light, with most stations recording a predominantly easterly component.

2) For a portion of the day (outlined by contours) the winds increased in speed from the southeast with the strongest winds along the immediate east coast decreasing inland to AA4.

3) After the period of substantial southeast winds (which varied in duration and time of termination depending on location), and away from the immediate east coast, the winds became quite irregular in speed and direction for approximately 1-2 h. Afterward, the winds became as light as in the morning but were more irregular in direction.

4) The region of significant southeast winds was found to correlate quite well with the time that the observed surface temperatures were greater than 28.8°C. (area enclosed by the dashed line in Fig. 6).

5) The regions of highest observed temperatures were found somewhat inland from both coasts, but well away from the interior. This is a feature we have observed on other time cross sections prepared from the FACE data for other dates.

The first three features of the time variation of the wind patterns described above [also found in the south

Florida surface wind maps in Cotton and Pielke (1976b)] can be explained in terms of the response of the surface layer to changes of surface heating due to shower activity and to the diurnal variation of insolation, as well as to accelerations caused by the heating of the air over land (the sea breeze). Using the observed 1000 mb potential temperature (28.8°C) from the 0700 LST Miami radiosonde sounding (see Cotton and Pielke, 1976b), it was possible to estimate the change-over from a stable to an unstable lapse rate in the surface layer in order to determine the importance of low-level stability on the winds.⁴ Once the layer becomes unstable, the surface winds should be representative of the large-scale pressure gradient,⁵ whereas when the layer is stably stratified the winds would be expected to be weak. As discussed under 4), the agreement between the onset and termination of significant southeast winds and the surface layer stratification is quite good and must be directly related to the development the later elimination of an unstable surface layer. In the morning, the regularity of the direction of the light winds suggests that the stabilization was due to cooling over a large area by radiation. In the afternoon, the more irregular wind directions and the occurrence of stronger variable winds for a short time after the termination of the southeast winds suggests that the

⁴ More precisely, of course, once the gradient Richardson number decreases below the critical value separating laminar from turbulent flow, the surface layer will be coupled with the atmosphere above. The adiabatic lapse rate, however, is not much different and is easier to compute than the Richardson number. Changes in the 1000 mb potential temperature due to the sea breeze circulation, which may be important, cannot be evaluated with such data.

⁵ Synoptic plus mesoscale pressure gradient.

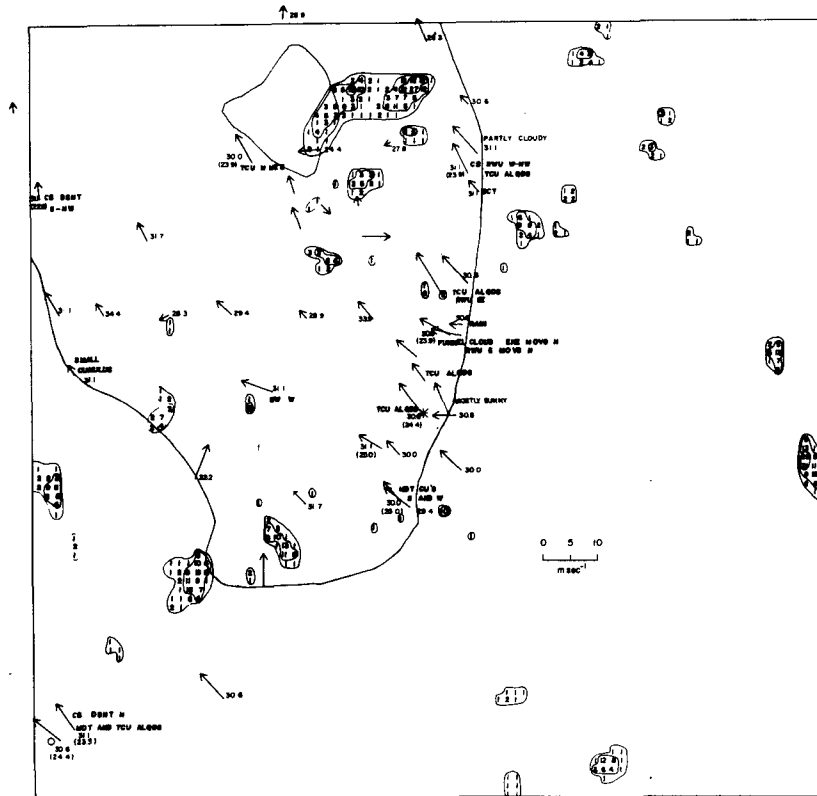


FIG. 7. The shower pattern observed from the Miami WSR-57 10 cm digitized radar along with surface wind observations for 1000 EST 4 August 1973. Comments regarding significant weather, station temperature ($^{\circ}\text{C}$) and dew point (in parentheses) are included at stations where they were available. The contour levels, as given by Herndon *et al.* (1973) correspond to 0.25, 2.29, 13.72, 30.23, 66.55 and 190.75 mm h^{-1} . The locations of showers relative to the Florida map base were obtained from Jane Eden of the National Hurricane and Experimental Meteorology Lab, who worked with the placement of the digitized shower echoes until they corresponded by eye with the photographs of the radar scope.

surface was cooled as a result of rain and cloud cover, as well as due to nocturnal cooling as the sun sets. The surface winds shown on the shower maps in Figs. 7–16 will illustrate further the influence of showers.

The development of maxima in temperature inland from both coasts (Fig. 6) may be related to the sea breeze convergence of heat [see, for example, Fig. 2, in Cotton and Pielke (1976a)]. In these convergence zones, not only is the temperature in the lower several hundred meters warmer than the surroundings, but the lighter winds at this time, which are indicative of the low-level convergence, will allow higher surface layer temperatures than would be expected if the winds were stronger.

The surface winds plotted on the digitized radar maps for the period 1000 to 1900 EST (Figs. 7–16) provide additional documentation of some of the results found in the cross sections⁶ and illustrate the

⁶ Radar coverage for 0700, 0800 and 0850 EST are given in Cotton and Pielke (1976b), but are not reproduced here because the information was not recorded digitally at EML and are available only as copies from microfilm.

strong diurnal nature of the convection. At 0700 EST very little shower activity was observed by the Miami WSR-57 10 cm radar. Beginning about 0800 and continuing until 1500, the area of rain coverage developed in two main areas. One was along the west coast and had a similar pattern to that found in earlier studies of the sea breeze for synoptically undisturbed days with easterly component synoptic flow [see, for example, Pielke (1974), pp. 134–135 and 137]. The second region extended from east of Lake Okeechobee, southwestward across south Florida. This region, also, appeared to have a pattern similar to that found in earlier studies of the sea breeze under synoptically undisturbed easterly component flow, although as we will show shortly this line of activity was coincident with a synoptic-scale line of convection which extended from off the southeast United States, and therefore cannot be indicative of sea breeze forcing alone.

The region of showers inland from the west coast propagated toward the southeast during the day. This motion, contrary to the synoptic winds at any level, appeared to be a combined effect of an eastward moving

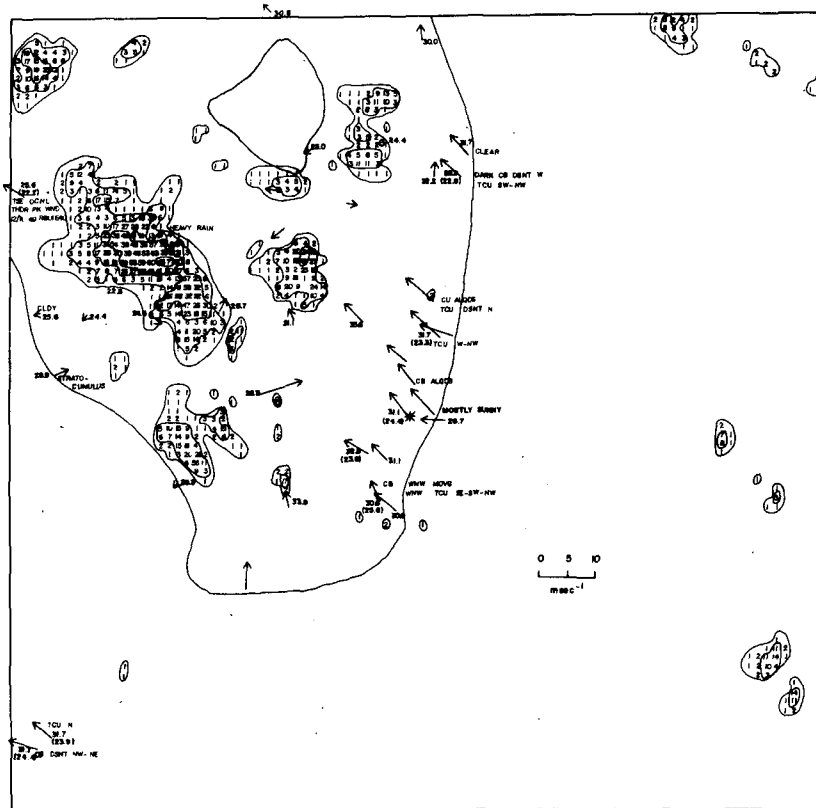


FIG. 12. As in Fig. 7 except for 1500 EST.

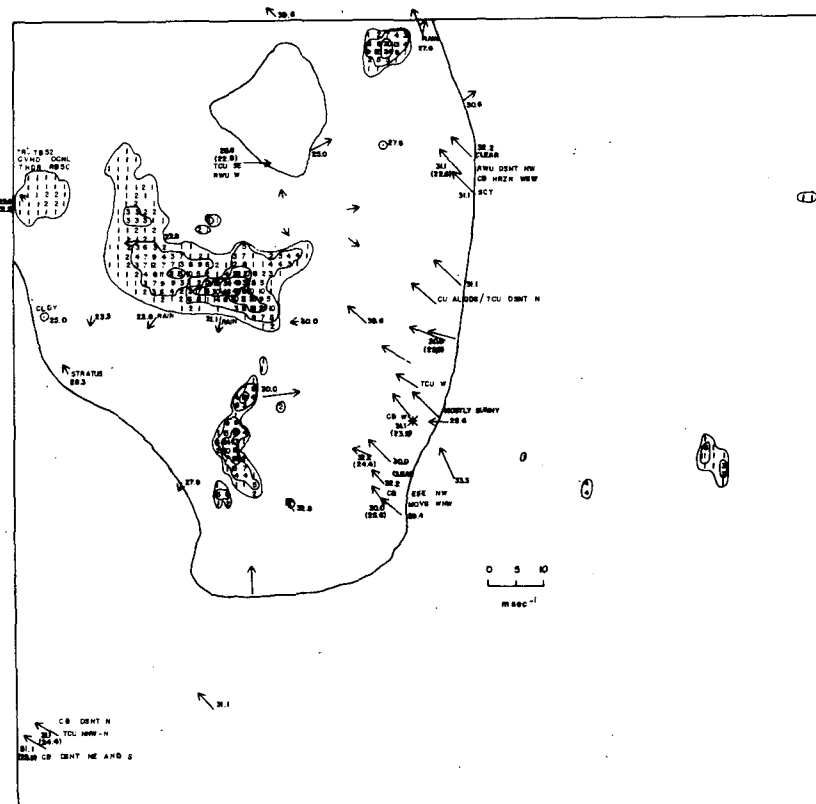


FIG. 13. As in Fig. 7 except for 1600 EST.

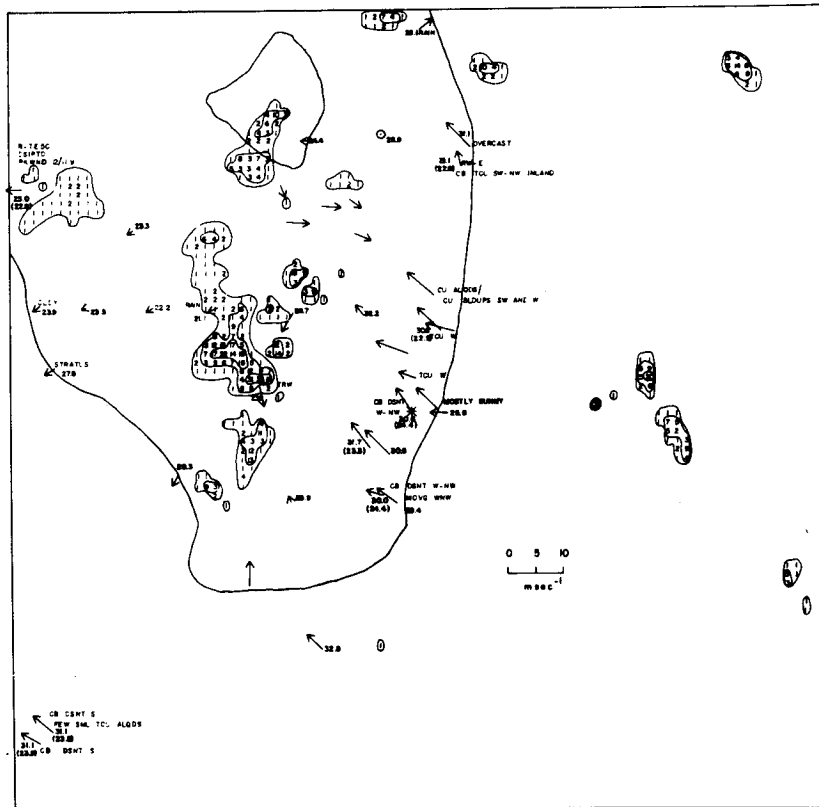


FIG. 14. As in Fig. 7 except for 1700 EST.

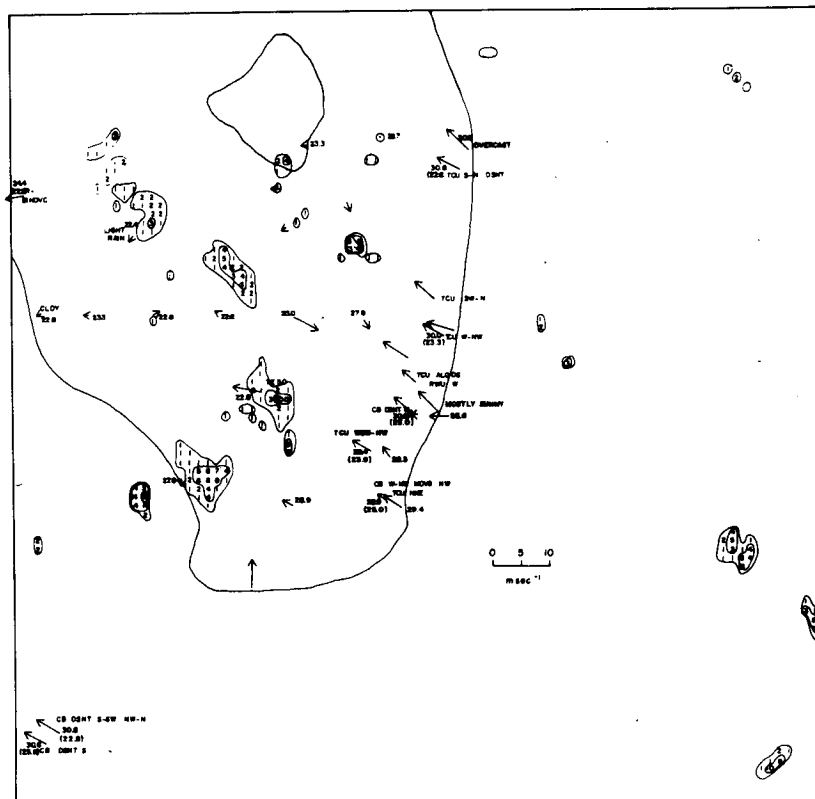


FIG. 15. As in Fig. 7 except for 1800 EST.

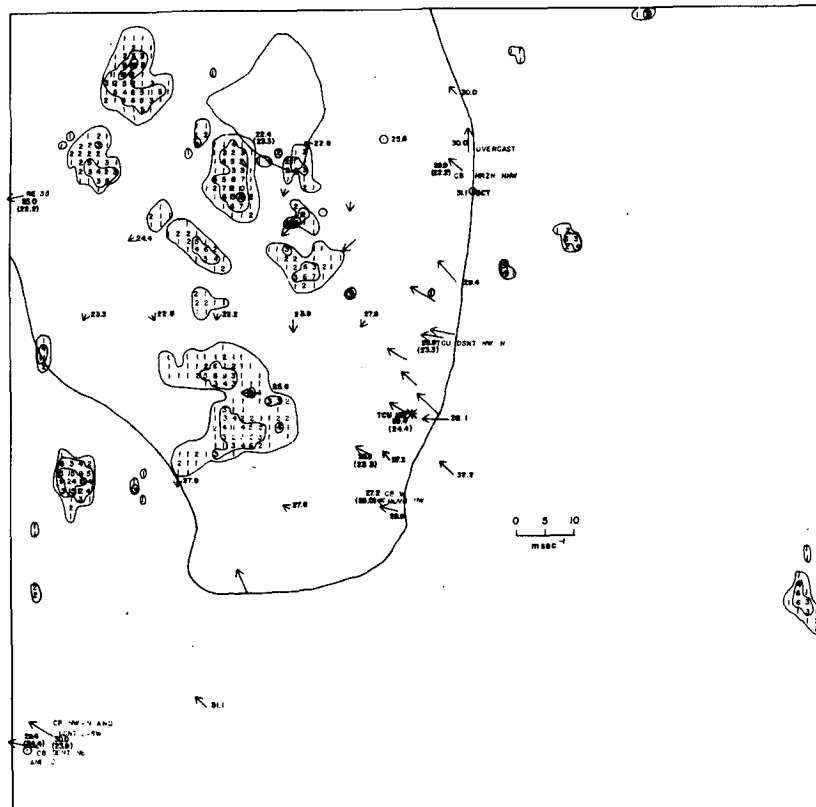


FIG. 16. As in Fig. 7 except for 1900 EST.



FIG. 17. DAPP satellite photograph at 1138 EST 4 August 1973.

sea breeze convergence zone, and a preferential development of the showers toward the area of synoptic-scale convection. After 1500 EST the shower activity decreased rather rapidly, although the rain which did occur appeared to prefer the two regions mentioned above. By 1800, as reported on p. 107 of Staff EML (1974), anomalous propagation became a problem, which by 1900, and continuing for the remainder of the night, was of moderate to strong intensity, thereby severely limiting the usefulness of the radar to detect showers.

One of the noticeable features of the spatial surface wind analyses is its remarkable uniformity along and somewhat inland from the southeast coast for the entire period shown. As was found in the cross section, the strengthened southeast winds had developed, apparently as a result of a sea breeze along with an unstable surface layer, near the time of maximum heating and then slowly decelerated later in the day. Significant surface convergence occurs inland from this area (from about 8 m s^{-1} to 4 m s^{-1} over a distance on the order to 50 km or so). If this convergence extended through a depth of 1 km, vertical velocities of 8 cm s^{-1} would result, although the aircraft flight at 610 m during the 1050 to 1136 cross section (Fig. 19) indicated divergence in the east-west component by that level over the area of low-level convergence. The observed wind pattern

is similar to that predicted by Pielke and Mahrer (1976) for another summer day in 1973 and, for that case, was attributable to accelerations due to the differential pressure gradient between land and water and because of the development of a superadiabatic lapse rate. Both mechanisms are due to diurnal surface heating.

Also evident in the analyses is the large variability of wind speed and direction in the vicinity of showers. Recently, Stan Ulanski (personal communication) found that the winds over the University of Virginia network (see Fig. 4) converge in low levels preceding a shower and then diverge at the end of its lifetime as downdrafts dominate the cumulus circulations. This pattern is seen several times in these analyses [for example, note the wind pattern in the upper western coastal area from 1200–1600 EST associated with a cumulonimbus complex. Inflow into this system is also seen in the 1210–1309 EST aircraft cross section (Fig. 20)].

The problem of anomalous propagation (AP) in the radar return became important starting about 1800 EST. As seen in Figs. 15 and 16, this corresponds to the time significant rainfall is ending and suggests that cooling of the ground by rain as well as nocturnal cooling as the sun sets have created the stable low level necessary for AP. Some of the analyzed shower area in Figs. 15 and 16 appears to be AP since TNT, for example, did not report rain in their remarks even though an echo was indicated over them.

The development of showers offshore from the southwest coast is unusual for a supposedly synoptically undisturbed day. The Data Acquisition and Processing Program (DAPP) satellite at 1138 EST (Fig. 17) shows that this activity was part of a well-defined region of cumulonimbus convection which stretched from northeast through southwest across south Florida. This activity was not continuous, but was broken into fairly regular masses of convection. The cirrus were shearing off toward the west or west-northwest, which is reasonably consistent with the 200 mb analysis (Fig. 3) except that no northerly component to the anvil would be expected. There was some evidence of cumulus development immediately parallel to the west coast. This last feature would be expected from the sea breeze, but the more extensive cumulonimbus development inland from the east coast seems indicative of a synoptic-scale disturbance.

The ATS-3 geostationary satellite documents the time history of this disturbance. As seen in Fig. 18 a well-defined line of clouds had developed as early as 1017 EST, and became more intense up until 1421 when the linear orientation broke down and was replaced by a preference for activity over south Florida. The line was visually connected to the bright cloud mass off the southeastern coast of the United States. As seen by the radar (Fig. 9), and as observed from

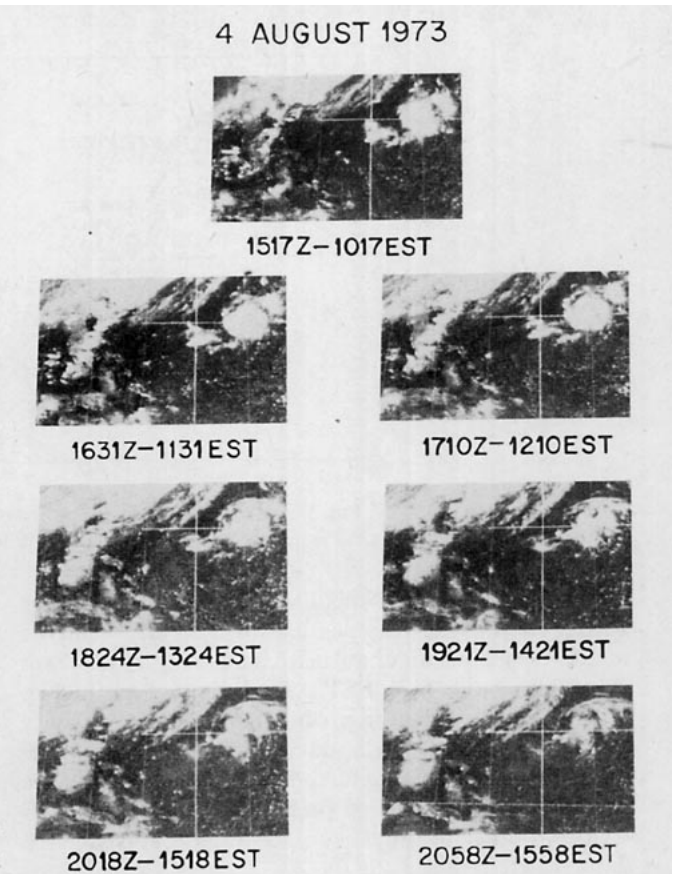


FIG. 18. Selected ATS-3 satellite photographs for 4 August 1973.

the cloud base aircraft (from 16 mm nose camera color film), much of the bright cloud mass viewed in Figs. 17 and 18 was nonprecipitating cirrus.

The synoptic analyses performed during the FACE program by Fernandez-Partagas (Appendix A of Staff, EML, 1974) indicated that 4 August 1973 was synoptically undisturbed. The synoptic analyses presented in Section 2a of this paper supports his conclusion, as does the strong diurnal nature of the convection and the patterning of the showers which suggests the concept of sea breeze forcing. Nonetheless, the satellite photographs document that a well-pronounced, synoptic-scale region of disturbed weather extended across south Florida, and was probably the reason for the relatively heavy rainfall in the EML target area on this date. The synoptic disturbance was not resolved in the synoptic analysis, apparently because it was offshore in a data-void region, while it was not seen in the early morning satellite photographs because either it was not very intense or it was a middle or upper level tropospheric disturbance which required the assistance of a low-level convergence field to make clouds. Surface heating of the land was therefore needed to generate the required upward motion at low levels over south Florida. Such a synoptic feature would be extremely difficult to predict, but its determination after the fact would be very useful in the post-operative

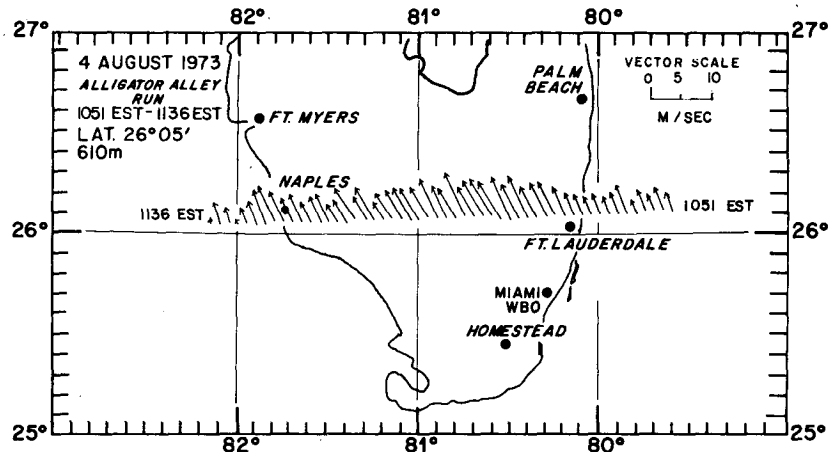


FIG. 19. Horizontal winds during the period 1051-1136 EST from an aircraft cross section at 610 m for 4 August 1973.

analyses of a weather modification program, such as FACE. It may also be possible to use early evidence of the development of such a cloud line, as seen, for example, by the 1131 EST ATS-3 photograph in Fig. 18, to provide a better predictor of cumulus activity for the remainder of the day. One could then superimpose the synoptic disturbed area on top of the sea breeze predicted area of preferred thunderstorm activity, in order to provide an accurate forecast for the date.

c. Selected aircraft analyses

The Research Flight Facility (RFF) DC-6 aircraft flew flights across the peninsula on 4 August, measuring basic meteorological parameters and certain turbulent fluxes. The most useful variables measured for the purposes of this paper, include the surface infrared (IR) temperatures from a Barnes PRT-5 IR sensor, horizontal winds via a Doppler navigation system, and vertical air velocity. Vertical air velocity was measured with the NOAA-Gust Probe system which has been

described by McFadden *et al.* (1970) and Brown *et al.* (1974). The system was referenced to the inertial navigation system in a manner similar to that of Bean *et al.* (1972). The primary aircraft patterns were east-west cross sections flown at an elevation of 610 m; this level was chosen because it was generally below cloud base over land and at, or just below, cloud base over water. The horizontal winds from the three flights on this date are shown in Figs. 19, 20 and 21. During the 1051 to 1136 flights, the winds were rather uniform from the southeast with velocities of about 5 m s^{-1} along the east coast and around 7.5 m s^{-1} further inland. As seen in Fig. 8, the southeasterly surface wind directions at 1100 over most of south Florida were also rather uniform. The increase of winds inland along the east coast indicate divergence which could be a result of either a developing sea breeze circulation or the synoptic disturbance we discussed in the last subsection.

The next cross section, made somewhat further north between 1210 and 1309 EST, was substantially different with slower southeasterlies along the east coast and

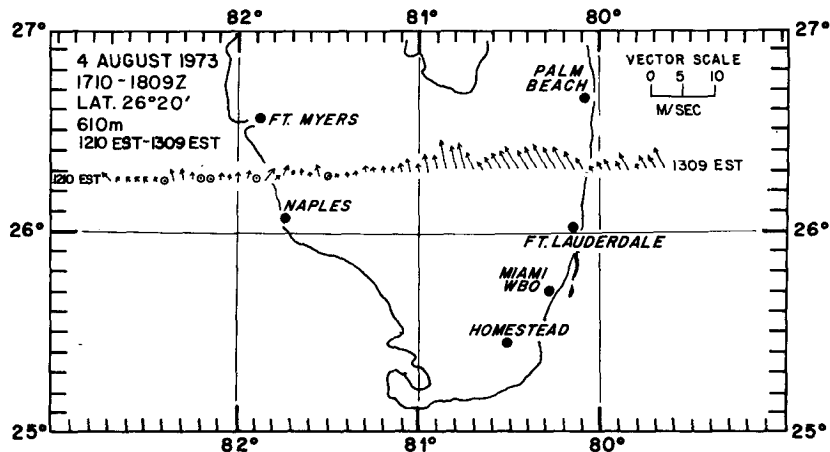


FIG. 20. As in Fig. 19 except for 1210 to 1309 EST.

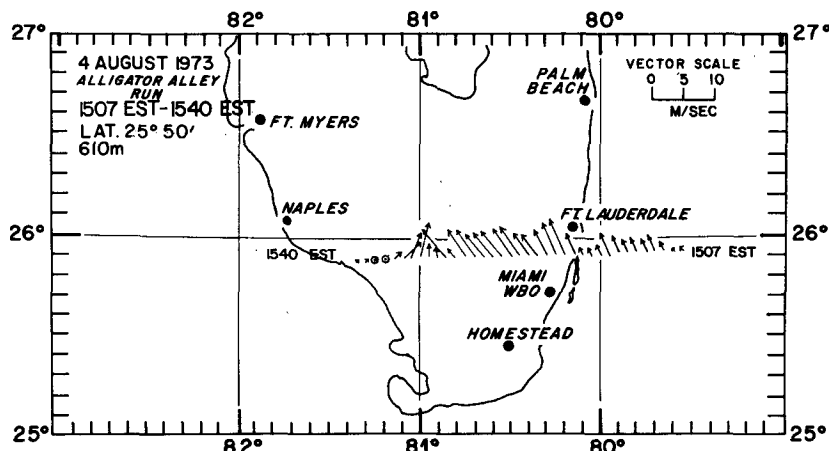


FIG. 21. As in Fig. 19 except for 1507 to 1540 EST.

very light winds further west. The pattern indicates three regions of substantial changes of the wind—near longitude 81°W, near longitude 80.6°W and immediately inland along the west coast—all of which are in the vicinity of showers as observed by the Miami WSR-57 radar (Figs. 9 and 10).

The final cross section of the day was made further south between 1507 and 1540 EST. The area of convergent winds around 81°W was, again, coincident with a region of showers, while the winds were rather regular out of the southeast, east of that area. The winds at this level accelerated from the east at the east coast.

From these three analyses only two conclusions are possible. On 4 August the winds at 610 m were rather irregular near the shower areas, but generally rather uniform elsewhere. Because of the nature of the observations, the occurrence of a shower before the convergent winds, or vice versa, could not be determined. Second, the winds for each cross section accelerated as the aircraft flew from water to land along the east coast.

Vertical air velocity was computed for the 1210–1309 run in the cross section illustrated in Fig. 20. An analysis of the vertical velocity data for the 1051–1136 EST run and the 1507–1540 EST run was not made because of serious recording errors. Fig. 22 illustrates the cross section of vertical velocity averaged over a record length of 11 km, observed at a height of 610 m from 1210 to 1309 EST. Each sample point represents a linear average over a record length of 11 km centered about the sample point. The data are so displayed in order to facilitate comparison with data predicted by the mesoscale model developed by Pielke (1974), and modified as reported by Mahrer and Pielke (1976) and Pielke and Mahrer (1975). It should be noted, however, that the mesoscale model data represent a volumetric average over a finite time scale, while these data represent a simple time series average interpreted to represent a linear spatial average assuming stationarity of the velocity field during each averaging segment.

As illustrated in Fig. 22, the vertical velocity is

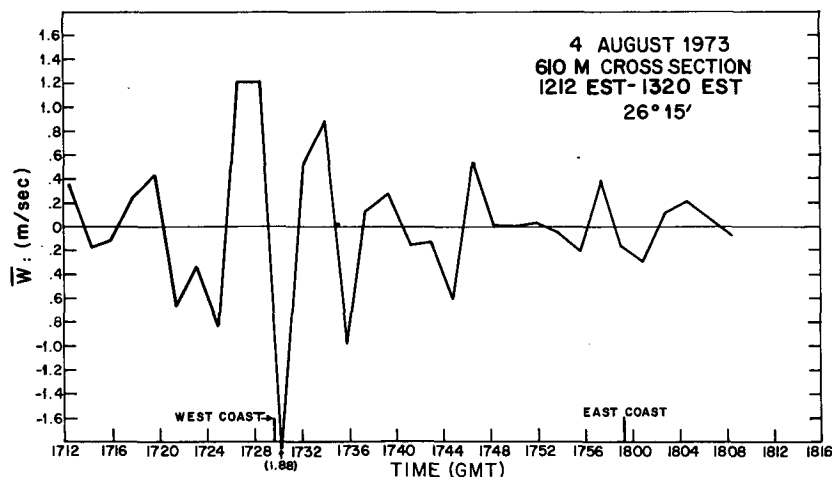


FIG. 22. Vertical velocities at 610 m averaged over 11 km across a section of south Florida from 1212 to 1320 EST 4 August 1973.

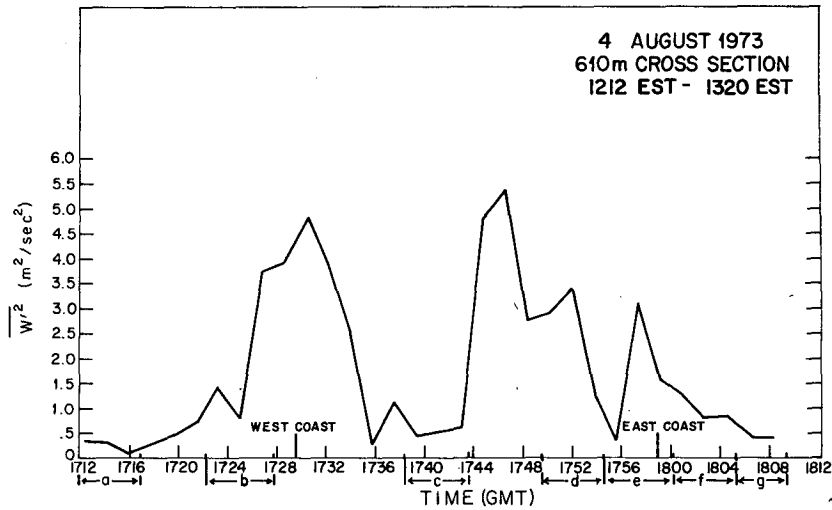


FIG. 23. As in Fig. 22 except for w'^2 .

weakly positive on the order of 20 cm s^{-1} over the Atlantic but becomes downward on the order of 30 cm s^{-1} as the coast is approached. A region of upward motion of approximately 40 cm s^{-1} can be seen along

the east coast followed by regions of zero to weak upward and downward motions in the center of the peninsula. As the west coast is approached the magnitude of average upward and downward vertical ve-

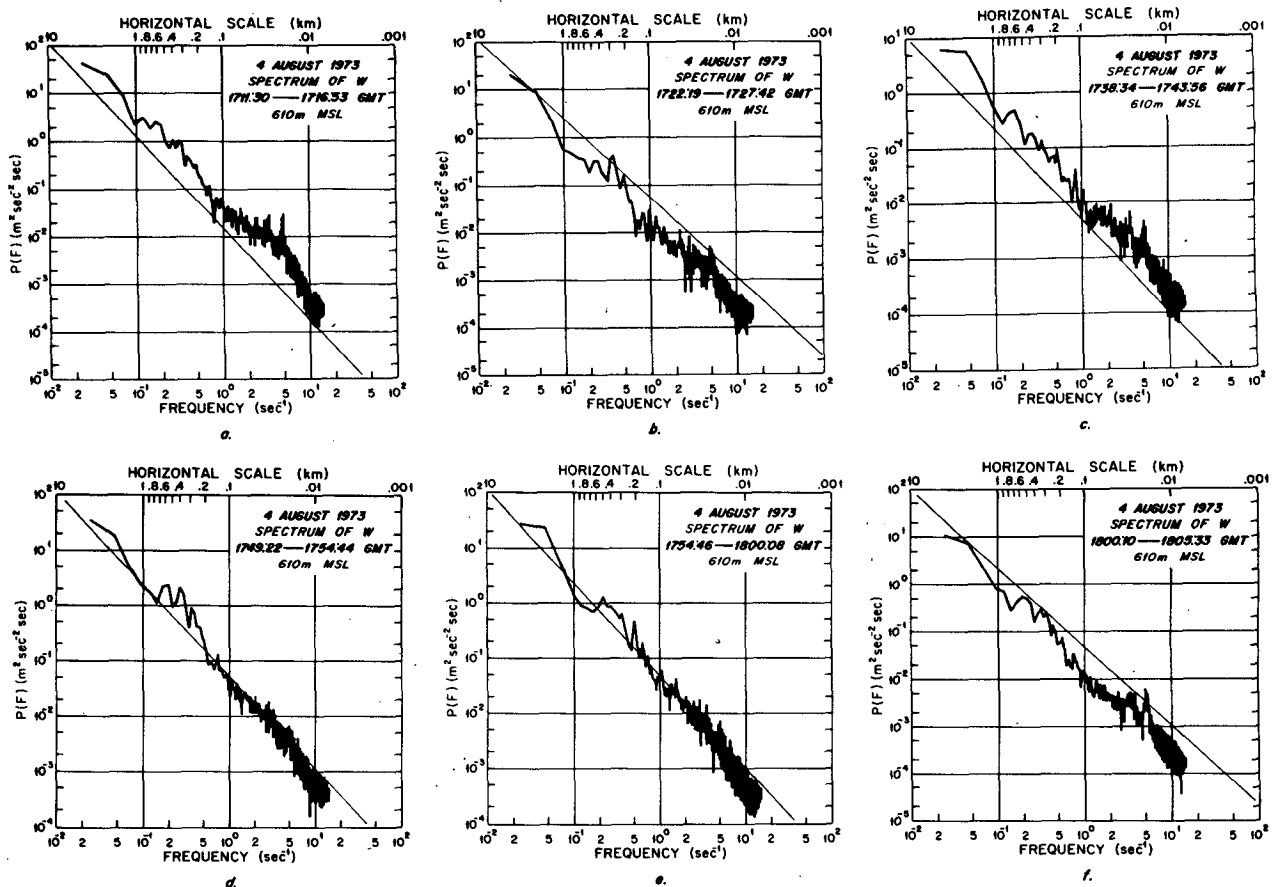


FIG. 24a-f. Energy as a function of frequency for the vertical velocity during selected segments of the aircraft flight, as indicated in Fig. 23.

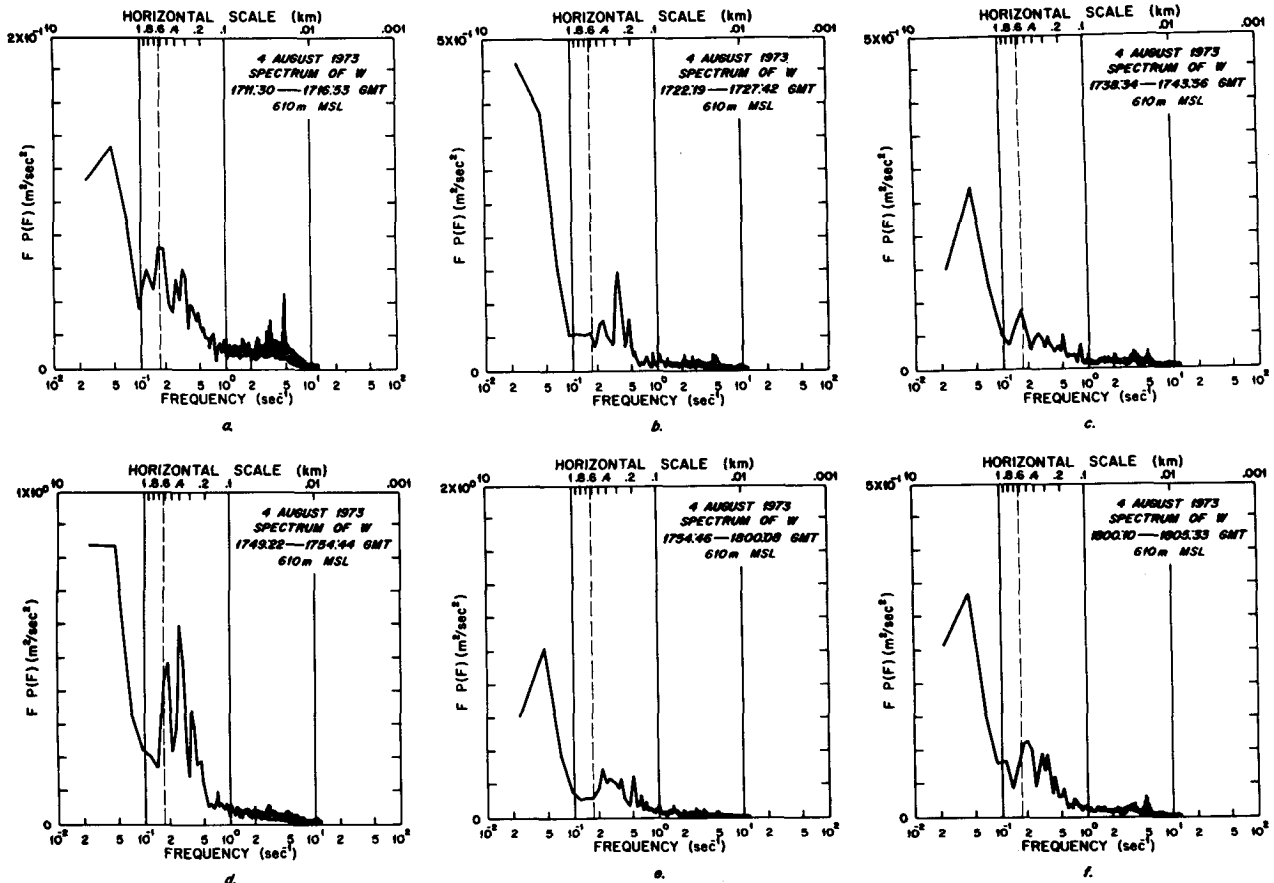


FIG. 25a-f. Frequency times energy as a function of frequency for the vertical velocity during selected segments of the aircraft flight, as indicated in Fig. 23.

locity increases to over 1.0 m s^{-1} . The largest magnitude is over -1.8 m s^{-1} , just along the west coast of the Florida peninsula. The largest positive vertical velocity occurs just off the west coast with a magnitude of 1.2 m s^{-1} . As shown in Figs. 9 and 10, this is a region of active cumulonimbus convection extending westward over the Gulf of Mexico. Of interest is the large point-to-point variability in average vertical velocity at cloud base. Along the west coast, for example, the mean vertical velocity varies by more than 2.0 m s^{-1} over a distance of only 11 km.

Fig. 23 illustrates the variance from the 11 km average vertical velocity discussed above. The region over the Atlantic is characterized by both weak mean vertical velocity and velocity variance. Over the east coast the variance increases in magnitude to $\sim 3.0 \text{ m}^2 \text{ s}^{-2}$, followed by a region of weak variance further inland. The central portion of the peninsula is characterized by strong variance in w exceeding $5.0 \text{ m}^2 \text{ s}^{-2}$ or a corresponding standard deviation of 2.2 m s^{-1} . As seen in Fig. 22 this region was characterized by mean upward and downward velocities up to 0.6 m s^{-1} . This region is also characterized by a few small radar echoes (Fig. 9 and 10). In comparison to the cumulonimbus systems

observed along the west coast, these cells are much smaller in extent and thus contribute less to the mean vertical velocity. The ratio of kinetic energy between the fluctuating and mean field ($\overline{w'^2}/\bar{w}^2$) over the central portion of the peninsula is approximately 14:1. On the other hand, over the west coast, where a broad region of variance as large as $4.8 \text{ m}^2 \text{ s}^{-2}$ can be seen, ($\overline{w'^2}/\bar{w}^2$) is only 1.45-2.8. This illustrates that this system is a larger scale system. The region of low variance in the west central portion of the figure correlates with the absence of showers as seen in Figs. 9 and 10.

To explore the partitioning of energy as a function of wavelength, power spectrum analyses were performed over selected blocks of the peninsula cross section made from 1210 to 1309. Each spectrum was computed over a finite time series corresponding to a spatial distance of 33 km [again similar to Bean *et al.* (1972)]. Mean values and linear trends in w were removed and the data were numerically low-pass filtered at 4.5 Hz. Figs. 24a-f illustrates the log-log spectra computed at positions a-f, illustrated in Fig. 23. Unfortunately, a complete set of power spectra was not computed for the west-east run because some of the

time series were contaminated with random noise introduced by problems with the digital recording system.

For reference, each of Figs. 24a-f has a line plotted having a $-5/3$ slope. In general, the spectra tends to follow this slope except for the strong secondary peaks in power in the scale range of 0.9–0.2 km. The secondary peak in power spectra is best illustrated in the region of intense vertical velocity variance shown in Fig. 24d. Strong excursions from the $-5/3$ slope occur at scales of 0.6 and 0.4 km. Such a spectral distribution is best illustrated in the $FP(F)$ spectra shown in Figs. 25a-f. The significant features of the spectra are a persistent trough in the spectra at 0.8–1.0 km with strong second-

ary peaks varying in scale from 0.2–0.8 km. The region of secondary maxima (0.2–0.8 km) is what may be called the "thermal convection" scale and appears to be distinctly separated from the microscale (scales <0.1 km). In a parallel analysis on 17 July 1973, we have found that the peaks in spectral density within the thermal scale range correspond well with the scales of cumulus and cumulocongustus observed during each leg of the run. Also illustrated for reference is a dashed vertical line in Figs. 25a-f, noting the height of the sample level. Thus, while a peak in the spectra within the thermal scale range often corresponds to the depths of the sample level, this scale is not always the maximum

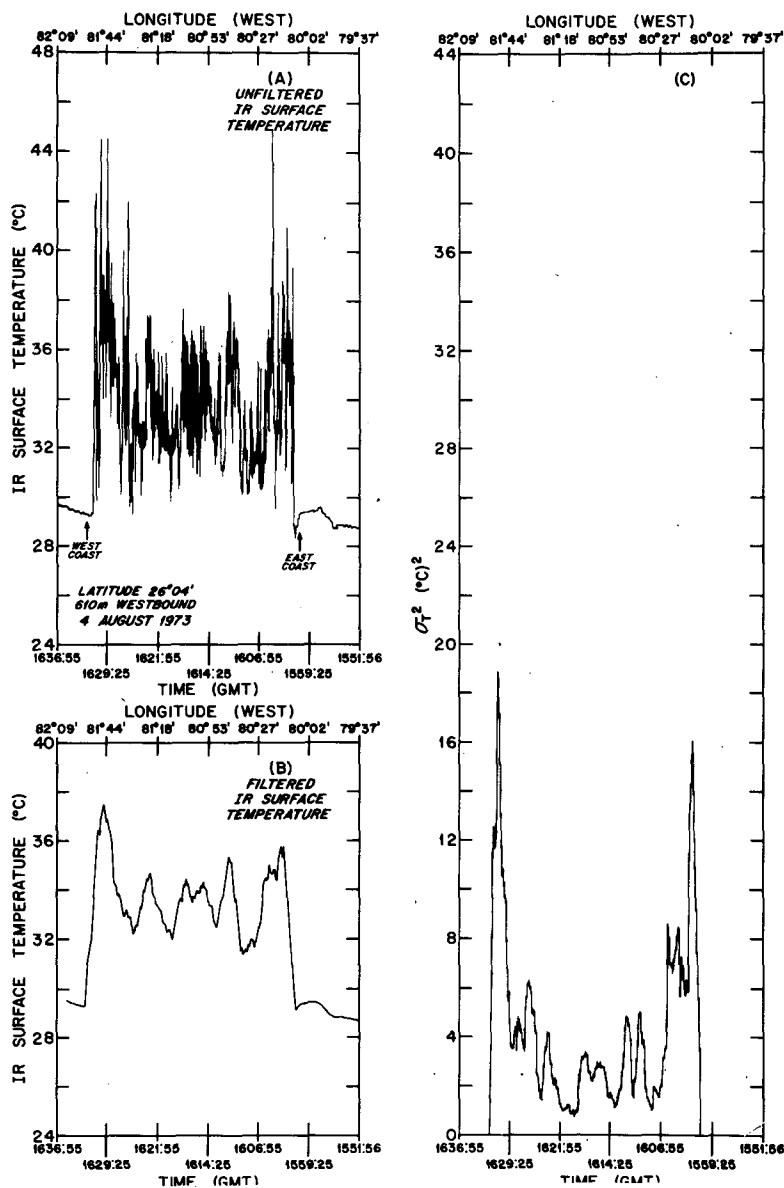


FIG. 26. Infrared surface temperature for the period 1051–1136 EST from an aircraft cross section for 4 August 1973: (a) unfiltered data, (b) 11 km averaged data, (c) variance with respect to 11 km averaged data.

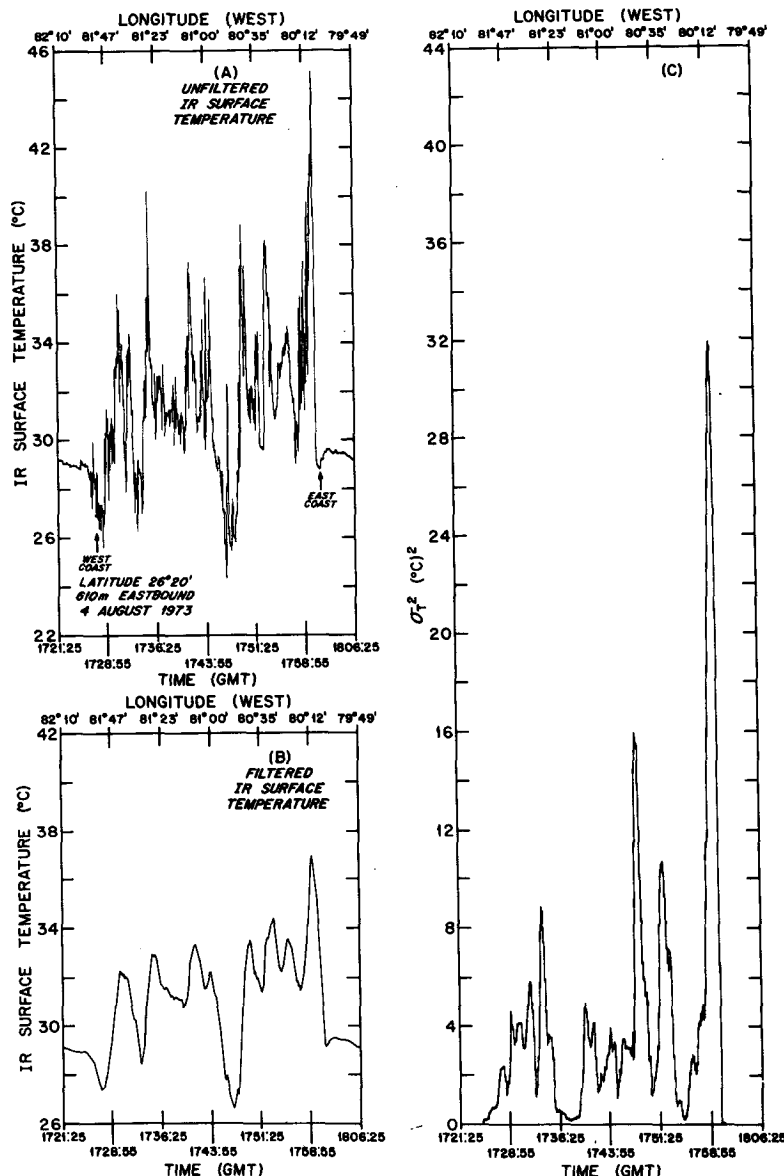


FIG. 27. As in Fig. 26 except for the period 1221–1306 EST.

energy-containing size within the thermal scale range, nor is it consistently a secondary peak. The reader should note that the ordinate scale varies in Figs. 25a–f.

The vertical velocity spectra and mesoscale averaged vertical velocity and its variance clearly illustrate the strong interaction between the thermal scale and the mesoscale. These analyses, furthermore, suggest there may be a well-defined scale separation between the thermal scale and the mesoscale. If the suggestion of an energy trough on scales of 0.8–1.0 km can be shown to be a consistent feature of convective systems, then such an observation would provide a physical justification for defining the resolution limit of mesoscale models to be on the order of 0.8–1.0 km. In so doing, however, it must be recognized that such a model should not be

closed with a simple eddy viscosity approximation, since the thermal convective scale range (the immediate subgrid scale) is a region of significant kinetic energy production.

The importance of the thermal scale range as a region of kinetic energy generation should not be surprising since, as we shall see in the analysis of surface temperature, there are strong fluctuations in surface temperature on scales less than 11 km.

Fig. 26a illustrates the cross section of surface temperature as digitally recorded at 1 s intervals from 1051 to 1135 EST. Since the raw data were rather noisy, it was decided to smooth the initial data by performing a running average over a length scale of ~11 km. Fig. 26b illustrates the smoothed IR data which show that

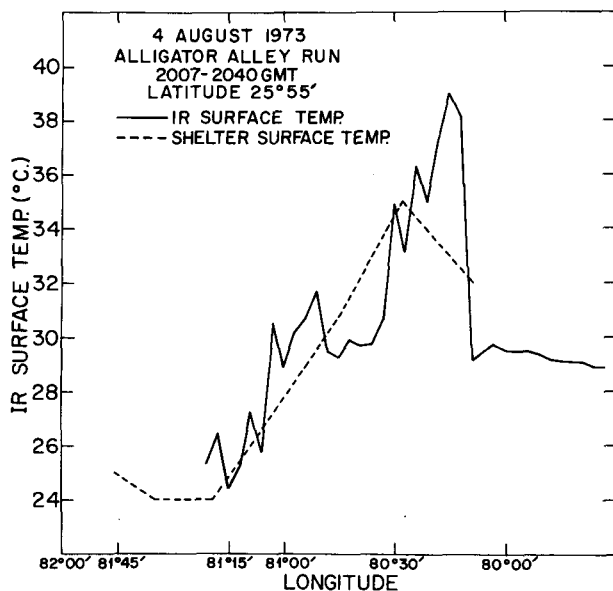


FIG. 28. Infrared surface temperature evaluated at 11 km intervals, for the 1507–1540 EST aircraft cross section for 4 August 1973.

the surface temperatures were generally warmer than the surrounding water by $\sim 5^{\circ}\text{C}$. The maximum amplitude of land-sea contrast occurred slightly inland from both coasts. The coastal areas are often open sandy areas as well as regions of maximum population density with the associated roads, concrete buildings, etc. Fig. 26c illustrates the computed variance of surface temperature with respect to the mean temperature illustrated in Fig. 26b. Not only are the coastal areas the region of maximum average land-sea contrast, but they are also the region containing the largest variance. In fact, the magnitude of the standard deviation of surface temperature in the coastal regions is comparable to the average land-sea temperature contrast. Other relative maxima of surface temperature are observed further inland, although with much smaller variances than nearer the coast.

A second cross section was made between 1221 and 1306 (Fig. 27). The IR temperature pattern in this run was quite irregular in the central regions of the peninsula because the aircraft passed through precipitation shafts and over regions covered by cloud or over surfaces cooled by precipitation. Interpretation of the IR data in precipitation shafts is not straightforward because the sensor responds both to airborne raindrops and to surfaces cooled by precipitation and ground shadowing. Again, we note the maximum land-sea contrast occurs along the coastal areas with the maximum variance along the east coast.

A third cross section of the day was made between 1507 and 1540 (Fig. 28). These data were manually plotted (the previous runs were computer plotted) in order to overlay linearly interpolated values of the shelter temperatures (from Fig. 6) observed approxi-

mately below the aircraft flight path. Both the shelter and IR surface temperature show the same pattern and are quantitatively in reasonably good agreement. As a result of rain and an extensive cirrus shield, the temperature over the western part of the peninsula had fallen sharply. The temperatures along the west coast were, in the mean over 11 km intervals, up to 5°C colder than the Gulf, while along the east coast the mean temperatures had risen to over 8°C warmer than the Atlantic waters. The migration of the cirrus shield toward the west by the easterly winds at 200 mb must have been important in shielding a wide area over the western part of the peninsula.

Thus it appears the showers, which are diurnally induced by surface heating, tend to eliminate themselves because of cooling of the surface by rain and by cloud shielding. In any complete numerical simulation of the mesoscale circulations on this date, both effects must be included.

3. Conclusions

The rather extensive meteorological data available on this date provided a unique opportunity to describe the mesoscale circulations which developed. As seen in the last section, on a day when the synoptic field was apparently steady in time, the surface and 610 m winds were substantially altered by the diurnal heating of the sun with its effects on surface layer stability and on the development of a sea breeze, as well as by the resultant cumulonimbus convection. The spatial variation of the winds was largest in the vicinity of showers but quite small elsewhere. On this day showers developed in two preferred areas: one along the west coast, probably caused by the sea breeze, and the other extending northeast-southwest across Florida, apparently in a previously undetected synoptic-scale disturbed area. The conventional synoptic analyses gave no evidence for this large-scale disturbed area. It is concluded that the high rainfall on this date was due to the superposition of a linearly oriented synoptic feature on top of the sea breeze convergence field.

The surface temperature distribution was influenced by anvils shielding the sun, by cooling from rainfall, as well as by the normal diurnal variation in sunlight. In the western half of the peninsula, where the most substantial rainfall occurred, the surface temperatures in the late afternoon fell below those observed offshore. Earlier in the day, before significant shower coverage occurred, the highest surface temperatures were found just inland from the coast, probably indicative of the urban buildup along the coasts. Other maxima of surface temperature further inland may be due to the sea breeze convergence of heat. The onset and termination of significant wind velocities at the surface were correlated very well with the occurrence of positive surface temperature anomalies which resulted in an unstable surface layer. When the surface layer became

stable due to cooling by rainfall, clouds shielding the sun or radiational cooling in the evening, the surface winds tended to decouple from the large-scale pressure gradient and became quite weak.

The analysis of vertical velocity spectra and meso-scale averaged vertical velocity and its variance clearly illustrate a strong coupling between the mesoscale and the thermal scale. The ratio of kinetic energy between the fluctuating field and the 11 km average field ($\overline{w'^2}/\overline{w^2}$) was found to vary from a high of 14:1 for cumulus congestus and small cumulonimbi to a low of 1.45:1 for a better organized cumulonimbus system. Spectral analysis of vertical velocity indicated a marked scale separation between the thermal convection and its larger scale. If such a feature can be shown to be a consistent feature of convective systems, then this would provide physical justification for employing a grid resolution in mesoscale models on the order of 0.8–1.0 km. It should be emphasized, however, that this does not mean that the subgrid scale could be parameterized in such a model with an eddy viscosity approximation. Indeed, the above analysis clearly demonstrates that the thermal scale is a region of significant kinetic energy generation.

Finally, the analyses of the 4 August 1973 FACE data has demonstrated the need for mesoscale resolution data, not only in the post-evaluation of weather modification programs but also in the forecasting of local weather.

Acknowledgments. The authors would like to acknowledge the assistance of Brad Bean, Gus Emmanuel, Ray McGavin and Richard Gilmer of the Boundary Layer Dynamics Group of NOAA for the help in setting up the NOAA Gust Probe system, and their assistance in the design of the experiment and data reduction. The NOAA Research Flight Facility provided the aircraft support, assisted in the operation of the basic meteorological instrumentation and reduced the basic meteorological data, while Fred Toepfer aided in the analysis of the turbulence data.

The authors also wish to acknowledge the encouragement and support of Joanne Simpson, William Woodley, Robert Sax, Victor Wiggert and Ron Holle in formulating and developing the surface network. José Fernandez-Partagas, Cecelia Griffith and Jane Eden graciously provided supplementary data such as synoptic analyses, satellite photographs and radar mappings. Their support was very valuable and the authors thank them.

The organizations and personnel who volunteered to make the cooperative observations, and without whose support the peninsula observation program could not have been carried out successfully are listed below:

Mr. Rose, CKT: WCKT-TV
Mr. Jeffrey Barber, ENG: WENG radio
Mr. Ronald Beckey, STU: WSTU radio

Mr. R. H. Hoelzl, TTB: WTTB radio
Captain J. H. MacDonald, MIB: U. S. Coast Guard, Miami Beach
Dr. Clayton M. Cook, EN2: Physician
Mr. C. D. Henderson, TUR, PEV, RIV, STL: Florida Power and Light Company
Mr. Bob Grove, WES: WEAT-TV
R. L. Paulsen, VEN: U. S. Coast Guard, Lorsta Venice
M. J. Trude, VEN: U. S. Coast Guard, Lorsta Venice
Mr. John C. Lotz, CCF: WCCF radio
Mr. James L. Hunt, HOM: Homestead General Aviation Airport
Mr. Phillip D. Thomas, NOG: WNOG radio
Ms. Betty Haigh, OKA: Okeechobee Airport
Mr. Timothy R. Murphy, BOC: Florida Airmotive, Inc., Baco Raton
R. L. Boyan, NQX: Naval Station Key West
Mr. Van Murphy, OK1: Florida Division of Forestry
Mr. David R. Elmore, Jr., GOU: Florida Division of Forestry
Mr. Curtis G. Strickland, ONC: Florida Division of Forestry
Mr. Terry Temples, GOU: Florida Division of Forestry
Mr. R. B. Wightman, Jr., NAP: City of Naples, Airport Authority
Mr. Oscar Espejo, MAR: Marco Island Airport
Mr. Richard D. Baker, PGD: Charlotte County Development Authority
S. Gossick, ANP: Avon Park Flying Service, Inc.
Mr. Don R. Monger, RIC: U. S. Naval Observatory

We also acknowledge observers at Coast Guard Stations, Fort Lauderdale, Fort Pierce, Riviera Beach and Lake Worth Inlet as well as others associated with the above people who made observations during the FACE program but whose names we do not know.

We would also like to thank the following individuals and organizations who permitted us to place mechanical weather stations on land under their jurisdiction:

Mr. Herbert P. Schall, Tilford Flying Service, Inc. (PHK)
Mr. Louis F. Gainey, Florida Game and Fresh Water Fish Commission (JWC)
Mr. John G. Krupilis, Central and Southern Florida Flood Control District (AA2, AA3, AA4, AA5)
Mr. Claude McClain, National Park Service (PHH and LMR)
Mr. R. W. Steven, Florida Department of Transportation (AA1)

We also thank the National Park Service for providing us free boat transportation to the Lostman's River Patrol Station in order to maintain weather station LMR and we gratefully acknowledge the help of Mr. Nils Friber, Mr. Doug Bowen and Mr. Jim Olson in undertaking that task. The boat and the help of a skilled ranger, usually Mr. Nils Friber, were provided

whenever it was needed. This close cooperation between the two federal agencies bodes well for constructive scientific work in the future in the Everglades National Park.

Mr. Brian Jarvinen of NHC and others in EML assisted in setting up and dismantling the mechanical weather stations.

This work was partially supported by the National Science Foundation under Grant ATM-74-12559 A01. The data were collected while the authors were employed for the Environmental Research Laboratories of the National Oceanic and Atmospheric Administration and the support of that agency is gratefully acknowledged. Ms. Evelyn Arnette performed the difficult task of typing our manuscript, while Barbara Dinsmore helped in typing the final version, and their effort is appreciated.

REFERENCES

- Bean, B. R., R. E. Gilmer, R. L. Grossman and R. E. McGavin 1972: An analysis of airborne measurements of vertical vapor flux during BOMEX. *J. Atmos. Sci.*, **29**, 860-869.
- Brown, W. J., J. D. McFadden, H. J. Mason, Jr., and C. W. Travis, 1974: Analysis of the research flight facility gust probe systems. *J. Appl. Meteor.*, **13**, 156-167.
- Byers, H. R., and H. R. Rodebush, 1948: Causes of thunderstorms of the Florida Peninsula. *J. Meteor.*, **5**, 275-280.
- Cotton, W. R., and R. A. Pielke, 1976a: Weather modification and three dimensional mesoscale models. *Bull. Amer. Meteor. Soc.*, **57**, 788-796.
- , and —, 1976b: Mesoscale analysis of 5 select days during the 1973 FACE experiment. [In preparation (available from NOAA, NHEML, Coral Gables, Fla. 33124).]
- , —, and P. T. Gannon, 1976: Numerical experiments on the influence of the mesoscale circulation on the cumulus scale. *J. Atmos. Sci.*, **33**, 252-261.
- Day, S., 1953: Horizontal convergence and the occurrence of summer precipitation at Miami, Florida. *Mon. Wea. Rev.*, **81**, 155-161.
- Gentry, R. C., 1950: Forecasting local showers in Florida during the summer. *Mon. Wea. Rev.*, **78**, 48-49.
- , and P. L. Moore, 1954: Relation of local and general wind interaction heat the sea coast to time and location of air-mass showers. *J. Meteor.*, **11**, 507-511.
- Gerrish, H. P., 1969: Preliminary characteristics of south Florida tornadoes in the summer of 1968. *Preprints Sixth Conf. Severe Local Storms*, Chicago, Amer. Meteor. Soc., 192-196.
- Herndon, A., W. L. Woodley, A. H. Miller, A. Samet and H. Senn, 1973: Comparison of gage and radar methods of convective precipitation measurement. NOAA Tech. Memo. ERL D-18, 67 pp. [Available from NOAA/ERL, Boulder, Colo. 80302.]
- Mahrer, Y., and R. A. Pielke, 1976: The numerical simulation of the airflow over Barbados. *Mon. Wea. Rev.*, **104**, 1392-1402.
- McFadden, J. D., C. W. Travis, R. E. Gilmer and R. E. McGavin, 1970: Water vapor flux measurements from ESSA aircraft. *Preprints Symp. Tropical Meteorology*, Honolulu, Amer. Meteor. Soc., BIII, 1-6.
- Pielke, R. A., 1973: An observational study of cumulus patterns in relation to the sea breeze over south Florida. NOAA ERL Tech. Memo. ERL-OD-16, 81 pp. [Available from NOAA, ERL, Boulder, Colo. 80302.]
- , 1974: A three-dimensional numerical model of the sea breezes over south Florida. *Mon. Wea. Rev.*, **102**, 115-139.
- , and Y. Mahrer, 1975: Representation of the heated planetary boundary layer in mesoscale models with coarse vertical resolution. *J. Atmos. Sci.*, **32**, 2288-2308.
- , and —, 1976: Verification analysis of a three-dimensional model prediction over south Florida for July 1, 1973. University of Virginia, Rep. No. UVA-ENU SCI-MESO-1976-1 [Available from R. A. Pielke, Dept. Environ. Sci., University of Virginia.]
- Plank, V. G., 1969: The size distribution of cumulus clouds in representative Florida populations. *J. Appl. Meteor.*, **8**, 46-67.
- Simpson, J., and A. S. Dennis, 1974: Cumulus clouds and their modification. *Weather and Climate Modification*, W. N. Hess, Ed., Wiley, 229-281.
- Staff, Experimental Meteorology Laboratory, 1974: 1973 Florida Area Cumulus Experiment (FACE) operational and preliminary summary. NOAA ERL Tech. Memo. ERL WMPO-12 [Available from NOAA/ERL, Boulder, Colo. 80302.]
- Woodley, W. L., A. Olsen, A. Herndon and V. Wiggert, 1974: Optimizing the measurement of convective rainfall in Florida. NOAA ERL Tech. Memo. ERL WMPO-18 [Available from NOAA/ERL, Boulder, Colo. 80302.]